INTERNATIONAL JOURNAL OF AUTOMOTIVE AND MECHANICAL ENGINEERING
ISSN: 2229-8649 e-ISSN: 2180-1606
VOL. 20, ISSUE 2, 2023, 10398 – 10410
DOI: https://doi.org/10.15282/ ijame.20.2.2023.06.0804

RESEARCH ARTICLE

Effect of Turning Parameter and Fiber Pullout on Machinability of Unidirectional EGFRP under Cryogenic Condition

Hazari Naresh and Chinmaya Prasad Padhy*

Department of Mechanical Engineering, School of Technology, GITAM University, 502329 Hyderabad, India

ABSTRACT - The non-homogeneous and anisotropic nature of composites poses challenges during machining, requiring the use of specialized cutting tools. GFRP materials were selected for their excellent elasticity, corrosion resistance, and high strength, making them ideal for applications in the aerospace and automotive industries. In this work, the surface quality of UD-GFRP composite bars during CNC machining in diverse machining conditions (dry, wet, and cryogenic) was investigated while considering the fiber-pullout issue. The UD-EGFRP composite materials have been machined with a polycrystalline diamond tool. The Taguchi-L9 orthogonal-array technique is used to investigate and further analysis. Three independent-variables feed rate, rotational speed or cutting speed, and depth of cut have been taken into account for their optimal design to get better machinability of EGFRP. This study also investigates the delamination criterion in composites and establishes the correlation between its input parameters and output responses. The findings revealed that cryogenic machining led to a notable improvement of 25.21% in surface roughness compared to the other lubrication methods. Also, the reduction from 84 µm to 34 µm in fiber-pullout signifies that cryogenic cooling effectively mitigated the occurrence of fiber-pullout.

ARTICLE HISTORY
Received : 20th July 2022
Revised : 20th June 2023
Accepted : 24th June 2023
Published : 30th June 2023

KEYWORDS
UD-EGFRP;
Cryogenic condition;
Fiber pullout;
Taguchi L9 array;
Surface roughness

1.0 INTRODUCTION

The composite materials (UD-EGFRP) have played a vital role for many purposes and are required to know their performance while machining. E-GFRP is chosen for its excellent elasticity, corrosion resistance, strength, and load resistance, making it ideal for aerospace and automotive applications. The E-GFRP typically has lower tensile strength and stiffness compared to S-fiber, but it offers higher resistance to corrosion and better cost-effectiveness. The specific choice between E-GFRP and S-fiber depends on the requirements of the project and the desired balance between performance and cost. According to Mohamed et al. [1], the material under consideration exhibits non-homogeneous and anisotropic properties, making it challenging to machine. Additionally, it has poor machinability characteristics. The research on industrial UD-GFRP composites is highly valuable, as the obtained results either support or justify the existing research gap effectively. Gupta et al. [2] focussed on the machining of composites involving several input variables, and among them, the feed rate of the tool has a significant influence on surface roughness, tool wear, and cutting forces. To optimize their results, the researchers utilized a traditional lathe machine and implemented principal component analysis (PCA). The study conducted by Kumar et al. [3] involved the use of unidirectional glass fiber-reinforced plastic composites and carbide cutting tools. In the research conducted by Lee [4], the machining of a specific kind of composite material was investigated. Castrol oil with a water-to-oil ratio of 6:1 was utilized as a coolant during the machining process.

Henerichs et al. [5] directed their attention towards three challenging tools; cubic boron nitride (CBN) inserts, single-crystalline diamond tool inserts, and poly-crystal diamond tool inserts. They conducted experiments and found that the single-crystal diamond tool outperformed the other options. The analysis by Davim et al. [6] concluded that the machinability of glasses/carbon fiber mixed-polymer composites falls into poor machinability material categories and also that machining them requires a significant amount of work. For a deeper analysis by Cheng [7], an understanding of mechanical performance with milling operations and multiple-regression analysis is suggested. However, the focus of the study was CNC machining. Davim [8] introduces the concept that composite machinability demands additional specialized research to widen its use has been reported, where the composite characteristics are affected by the fiber length. Arul et al. [9] studied the quality of machining of GF reinforced-polymers with a specialized tool. However, this research focused on the use of a fluid with a CNC turning machine to enhance machinability in large-scale production while maintaining extreme accuracy.

The research by Işık et al. [10] focused on the machining of GFRP using stronger PCD and cemented-carbide inserts. The work by Mohd et al. [11] highlights sustainable manufacturing as a methodology that promotes a conducive working environment for employees protects the environment, and brings economic advantages to businesses. A sustainable production line aims to preserve the environment while also providing financial benefits. In their research, Hegab et al. [12] concentrated on conducting structural, physiological, and endurance tests in compliance with international standards.

*CORRESPONDING AUTHOR | Chinmaya Prasad Padhy | ✉ padhy.gitam@gmail.com

These tests aimed to evaluate the design and development of using matrices in the study. Experiments have shown that GFRP bars can provide a high degree of thermal conductivity while keeping consistent mechanical and physical properties. Simone et al., Sina et al., and Wan et al. [13-15] investigated the influence of various machining parameters, particularly feed rate, on fiber-pullout, delamination, and subsequent surface quality characteristics. The study also emphasizes surface roughness as a significant quality parameter. Singh et al. [16] conducted a study focused on optimizing operational variables, tool shape, and mathematical modeling to analyze and optimize the maximum thrust force in machining operations. In his research, he discovered that GFRP composite materials have been examined using Finite Element (FE) analysis, and the FE results have shown a strong correlation with experimental data. In the experimental investigation and optimization study on machining GFRP composites conducted by Palanikumar et al., Ugur and Ibrahim [17-19], significant insights and findings were obtained. Their research contributes to the understanding and improvement of machining processes in GFRP composites. Hazari et al. [20-22] explored the machinability of UD-GFRP composites under green-machining and cryogenic-machining environments. The study employed the RSM (Response Surface Methodology) and Taguchi technique to analyze and optimize the machining process. The research provides valuable insights into the machining of UD-GFRP composites. A study by Bin et al. [23] explored the chip formation mechanisms and chip morphology during composite machining and investigated the impact of cutting parameters on chip thickness, curling, and chip evacuation. Elfarhani et al. and Shyha et al. [24-25] investigated the thermal aspects of edge trimming in bio-filled GFRP, analyzing the impact of fiber orientation and silica sand filler on heat generation; valuable insights were gained regarding the thermal behavior during edge trimming operations.

Though many researchers engaged and contributed various theories by experimenting with improvising the machinability of GFRP, however, there are very limited studies available that focus more specifically on the E glass fiber pullout problems that arise in UD-GFRP. Hence, it is essential to study the machinability of UD-EGFRP to improvise the machining performances. The machinability of GFRP depends on several factors, including the specific composition of the GFRP, fiber orientation, tool selection, cutting parameters, machining environment, delamination control and post machining operations. This study investigates majorly the effect of fiber pullouts on the machinability (surface roughness) of a UD-EGFRP under cryogenic machining conditions, which explores investigating fiber pullout and chip morphology's effects on its surface roughness. A DOE (linear method) is used for experimentation, while RSM (nonlinear method) creates a mathematical relationship. The primary goal is to minimize fiber pullout and improve surface roughness. The experimental values are compared and validated against the mathematical relationship to assess the accuracy and reliability of the developed model.

2.0 METHODOLOGY

The investigation is focused on the quality of machining surfaces, including cutting forces. Turning operation is performed on the composite rod under diverse machine conditions (dry, wet and cryogenic) with the help of the Taguchi method. The Taguchi L9 array provides an evenly distributed combination of factor-level pairs and efficient estimation, making it suitable for screening experiments with a small number of factors (e.g., 3 in this case), the minimum number of levels is calculated with the formula (1) where E_{min} is the minimum standard of trials required is, F_{CF} specifies the number of variables that can be controlled and L is the level taken into account for each adjustable parameter. The contribution-parameters are considered as cutting speed (N), feed (f) and depth of cut (doc). The input parameters are shown in Table 1 and Table 2. Machining is done under dry condition, wet condition with the lubricating oil (VEEDOL ST 69) and cryogenic environment condition i.e. for cryogenics, liquid-nitrogen (LN_2) is employed for coolant. The liquid-nitrogen is eco-friendly, moreover colourless, tasteless, and abundantly available in the environment. The work methodology diagram of the complete experimentation is presented in Figure 1.

$$E_{min} = (\mathrm{L} - 1)\ \mathrm{X}\ F_{CF} + 1 \tag{1}$$

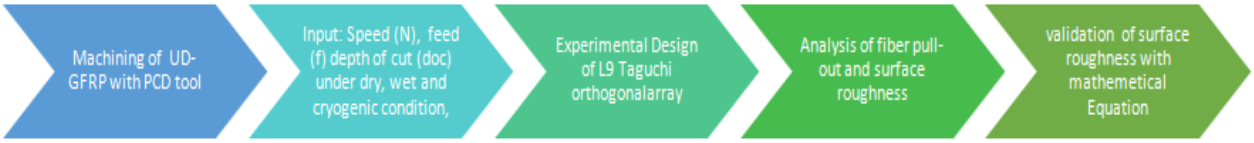

Figure 1. Work methodology

Table 1. CNC turning operating parameters ranges

Variable of process	Low	Medium	High
Speed in rpm	1000	1200	1500
Tool- feed rate in mm/ rev	0.05	0.1	0.15
Cutting - depth in mm	0.50	1.0	1.50

Table 2. Process parameters that are both independent and fixed

Independent process variables	Low	Medium	High
Cutting-environment	Wet condition	Wet condition	Wet condition
Condition tool-material	PCD	PCD	PCD
Tool rake-angle in degrees	6	6	6

3.0 EXPERIMENT

The E glass fiber composite (EGFRP) in turning operation with Taguchi L9 orthogonal array is made. The UD-GFRP composite rod (diameter of 20 mm and length of 150 mm) was taken for machining; the properties of composite and E glass are shown in Table 4. The PCD tool specifications are shown in Table 3. The machining operation is done with the help of a CNC lathe machine, as shown in Figure 2(a) and 2(b), and PCD tool, as shown in Figure 2(c). After machining, the composite bar was sent to measure surface roughness, shown in Figure 2(g) and the PCD cutting tool was sent to the tool maker microscope to measure the desired tool wear, as shown in Figure 2(f). While doing machining operations, the respective cutting forces were recorded with the assistance of strain gauge dynamometer, shown in Figure 2(e). The coolant is supplied through a hose pipe, as in Figure 2(d) and machined samples are shown in Figure 2(h). The dry wet and cryogenic machining were done according to the scheduled L9 TAGUCHI combinations, and results are shown in Table 5.

(a) CNC supper jobber 500 turning

(b) 3-jaw chuck with GFRP rod diamond insert

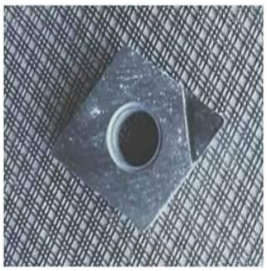

(c) polycrystalline

(d) coolant supply

(e) dynamometer microscope tester

(f) tool maker microscope

(g) surface roughness

(h) machined samples

Figure 2. Glass fiber reinforced polymer (GFRP) machining

Table 3. PCD tool specifications

	Properties of PCD tool.
Clearance-angle	6°
Grade	M10
Density	3.80-4.50 g/cm^3
Young's modulus	800-900 GPa
Thermal conductivity	150-550 W/m K
Compressive strength	7000-8000 N/mm^2
Cutting edge inclination angle top	6°
Tool rake angle	6°

Table 4. Properties of composite bar

Description of composite	Quantity/ Specification
Strength at compression	600 N/mm^2
Young's modulus	320 N/mm^2
Fiber-orientation	unidirectional
Epoxy-resin (by weight)	25 ± 5 %
wt.% of glass fiber contribution	75 ± 5%
Tensile-strength	650 N/mm^2
Strength at shear	255 N/mm^2
Agent of reinforcement,	Roving: E-glass
Properties of 'E' Glass	
Diameter	10-20 μm
Deformation	3.3-3.5 %
Young's modulus	68 GPa
Poisson's ratio	0.19
Specific weight	2.54 g/cm^3

Table 5. Taguchi L9 design of experiment (DOE)

Exp No.	Cutting speed(rpm)	Cutting speed (mm/rev)	Feed rate (mm/rev)	Depth of cut (mm)	Machining condition	Surface roughness (Ra)
1	1000	0.15	0.05	0.5	Dry	5.074
2	1000	0.15	0.10	1.0	Dry	5.692
3	1000	0.15	0.15	1.5	Dry	5.328
4	1200	0.12	0.05	1.0	Dry	5.751
5	1200	0.12	0.10	1.5	Dry	4.958
6	1200	0.12	0.15	0.5	Dry	6.436
7	1500	0.10	0.05	1.5	Dry	5.110
8	1500	0.10	0.10	0.5	Dry	4.580
9	1500	0.10	0.15	1.0	Dry	6.286
10	1000	0.15	0.05	0.5	Wet	4.958
11	1000	0.15	0.10	1.0	Wet	5.269
12	1000	0.15	0.15	1.5	Wet	5.126
13	1200	0.12	0.05	1.0	Wet	5.512
14	1200	0.12	0.10	1.5	Wet	4.648
15	1200	0.12	0.15	0.5	Wet	5.950
16	1500	0.10	0.05	1.5	Wet	5.101
17	1500	0.10	0.10	0.5	Wet	4.265
18	1500	0.10	0.15	1.0	Wet	5.901
19	1000	0.15	0.05	0.5	Cryogenic	3.985
20	1000	0.15	0.10	1.0	Cryogenic	4.213
21	1000	0.15	0.15	1.5	Cryogenic	4.124
22	1200	0.12	0.05	1.0	Cryogenic	4.289
23	1200	0.12	0.10	1.5	Cryogenic	4.098
24	1200	0.12	0.15	0.5	Cryogenic	4.258
25	1500	0.10	0.05	1.5	Cryogenic	4.085
26	1500	0.10	0.10	0.5	Cryogenic	3.925
27	1500	0.10	0.15	1.0	Cryogenic	3.826

4.0 RESULTS AND DISCUSSION

In the case of E-GFRP composites, one significant failure mode occurs when the adhesion between the layers (both interlayer and with the matrix) weakens, leading to substantial separation and degradation of the reinforcement layers. This failure mode is exacerbated in composite materials with low material quality, resulting in poor assembly tolerance and an increased risk of failure in the fractured zone. It is necessary to evaluate degradation throughout the machining process based on the results of experiments under dry, wet and cryogenic environment conditions for good quality at a lower tool-wear rate and surface finish. The surface-finish and tool-wear resistance are influenced by the damage criteria. From the results in Table 5, surface irregularity during machining in a dry environment is 5.46 μm (from an average of 9 experimental trials). It is depicted that surface roughness value gradually decreases from dry machining conditions to cryogenic, as there is a decrement (5.04%) of surface roughness value while moving from dry to wet conditions, and there is a significant decrease (25.22%) in roughness value is observed in cryogenic machining condition as compared to dry machining condition, whereas fiber pullouts are more prominent in dry machining (Figure 3).

Figure 3. Fibre pullouts during machining operation

Figure 4. Powder forms of chips in machining operation

During dry machining operations, chips are produced as fine powder dust (Figure 4) when the cutting tool interacts with the workpiece material. Additionally, in certain cases, fibre pullout can occur, as depicted in Figure 5. Fibre breaking is generally caused by the buckling and bending of straight fibre (Figure 6). This phenomenon involves the partial or complete extraction of fibres from the material's surface during machining. As a consequence of fibre pullout, the surface quality may deteriorate, leading to the formation of a rough surface.

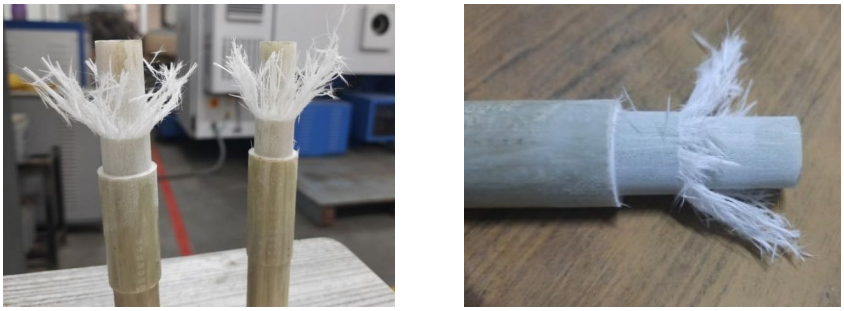

Figure 5. Fiber pullout under dry machining condition

Figure 6. Buckling and bending failure of fibres

It is to be noted that during dry machining, temperatures are acquired at the cutting edges and surfaces as well, resulting in increased tool wear and poor surface quality, whereas cutting fluids are used to improve cutting conditions by performing activities such as corrosion inhibition, lubrication, and chip cleansing, also lowering the temperature in the deformation zone. While cryogenic machining, often known as green machining, is a method of reducing tool wear by maintaining the temperature as low as possible during the machining process.

During machining, nitrogen fluid (LN_2) is used as a cryogenic cutting coolant to keep the cutting area cool. Compared to standard liquid oil-based coolants, LN_2 is a much more environmentally friendly cutting fluid. CO_2 has also become popular as a cryogenic coolant and a potential substitute for LN_2, having a greater melting point. However, it is cooled sufficiently to remove temperature from the cutting region, although it is not environmentally friendly. LN_2 is often

utilized as a cutting fluid and is stored in closed cylinders at constant pressure. In ambient settings, it boils at -196°C, maintains the heat lost in the cutting region, and evaporates without leaving any residue on the cutting tool or workpiece. Figure 7(a) clearly shows there is a reduction of fiber pullout; almost nil as in Figure 7(b) while machining under cryogenic condition. This is due to possible reasons like, might be maintained minimum cutting temperature and least or no heat generation while machining. Also, the application of cryogenics at the cutting zone can cause a transformation of the fibers from a ductile state to a more brittle state. This transition leads to the production of proper fiber shavings, which in turn results in improved surface finish and reduced tool wear.

(a) (b)

Figure 7. EGFRP cryogenic (a) machining and (b) machined samples

The scanning electron microscope is utilized to find out the details of fiber de-bonding and hence fiber pullouts. Here, Figure 8 represents the SEM image of an EGFRP surface while machined under dry conditions, where fibers are pulled out from the workpiece surface by buckling phenomenon as mentioned earlier and measured as 84 µm in length (approx.), which is visible over its entire surface of the periphery. This causes a higher fraction of surface damage, leading to higher wear of the tool, which increases the cutting force, consequently decreasing the tool's life and increasing the surface roughness.

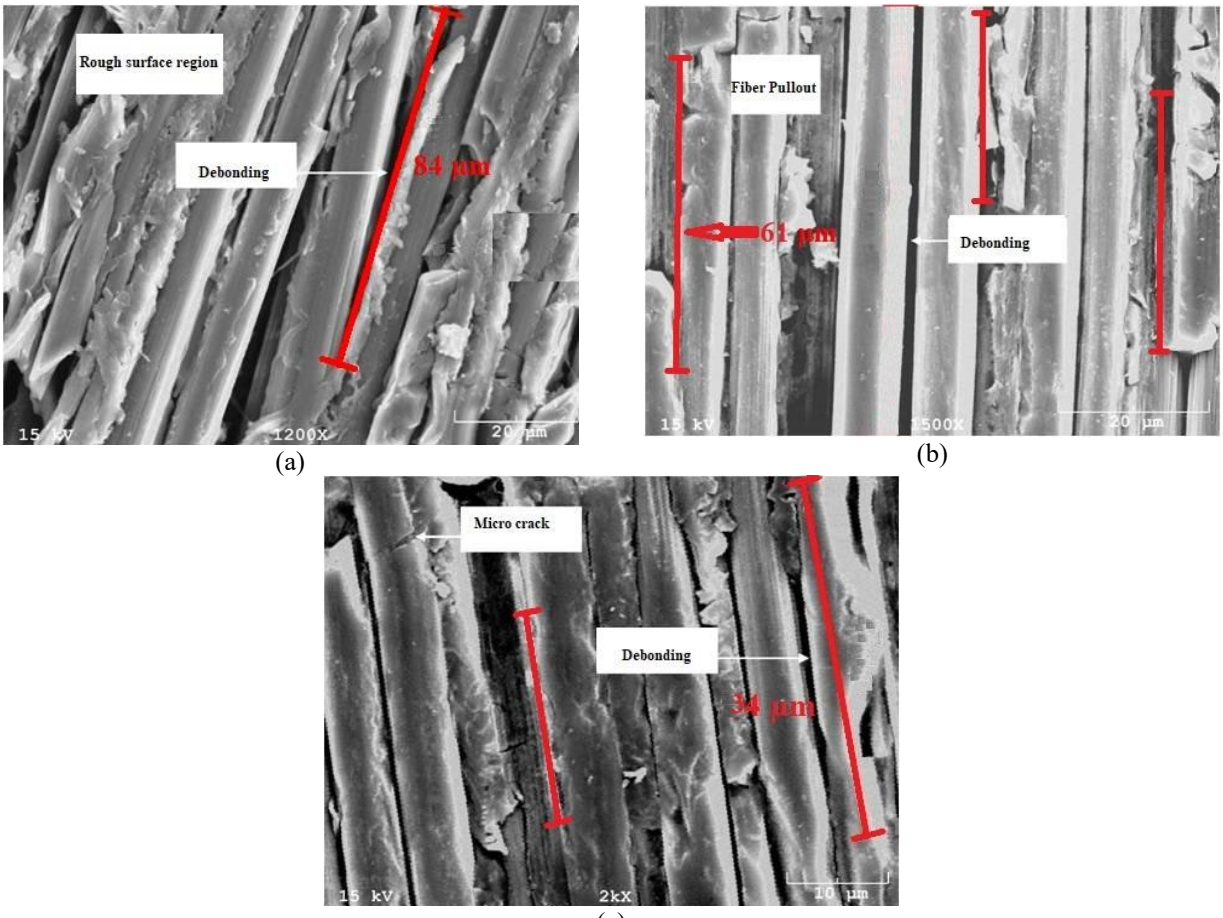

(a) (b)

(c)

Figure 8. Delamination observation under (a) dry condition and (b) wet condition and (c) cryogenic machining condition

In the case of wet machining conditions, the SEM image in Figure 8(b) shows a considerable breakage fiber length of 63 µm (approx.), which still causes the fiber pullouts and rough surface. Figure 8(c) indicates that fibre damage initiates

from lengths as short as 30 μm (measured from SEM image). This observation suggests that when fibres break in shorter lengths as compared with dry machining, also buckling occurs over shorter distances. As a result, this phenomenon contributes to a decrease in surface roughness values, indicating a favourable surface finish. This concludes the cryogenic environment conditions result in shorter length failures of the fibres, without causing surface damage near the pullout area or affecting the work material. Moreover, in this cryogenic environment, no liquid infiltrates the material where fibre pullout occurs, and there is no need for a specific time to dry out the work material post-machining. The cryogenic liquid evaporates under ambient conditions upon contact with the cutting tool and workpiece. Thus, this approach solely aims at enhancing the quality of machining operations required for EGFRP.

5.0 PREDICTIVE MATHEMATICAL MODEL FOR SURFACE ROUGHNESS

The prediction of fiber pullout serves as a crucial objective, which can be achieved by analyzing surface roughness parameters. Surface roughness is directly influenced by the occurrence of fiber pullout. By reducing fiber pullouts, surface roughness can be effectively controlled. As mentioned earlier, the response surface methodology (RSM) technique has already been discussed in relation to surface roughness. This technique plays a significant role in understanding and optimizing surface roughness in the context of fiber pullout analysis.

Certain adjustable parameters that influence response characteristics and also optimum processing conditions will indeed be considered [26]. The estimated values are controlled from bottom to top between allowed ranges, as per the tool manufacturer's catalogue. The temperature (t) ranges were considered for diverse (dry, wet and cryogenic) machining conditions as 40 °C, 28 °C and 1 °C.

$$\text{Spindle-speed } v_{\min} \le v \le v_{\max} \tag{2}$$

$$\text{Feed } f_{\min} \le f \le f_{\max} \tag{3}$$

$$\text{Depth of cut } d_{\min} \le d \le d_{\max} \tag{4}$$

$$\text{Temperature } t_{\min} \le t \le t_{\max} \tag{5}$$

Based on response surface methodology (RSM) - in general, to build a mathematical model, the displayed relation Eq. (6) should be used commonly. The below relation is commonly used for representing the mathematical models:

$$Y = \psi\ (v, f, d, t) + \epsilon \tag{6}$$

where Y is the response of the turning, ψ Is the "response--function" and v, f, d, t are the cutting-speed/velocity, feed rate, cutting-depth and temperatures. In general, ϵ is the error and is normally distributed mean of zero - based on the responses.

In general, ϵ is the error and is normally distributed with a mean of zero - based on the responses. Four major machining factors, such as cutting speed/velocity (v), feed rate (f), depth of cut(d), and temperature (t), have been used to explore the influence of machining parameters on surface roughness(Ra). These machining parameters were chosen as dependent input variables in this investigation.

To validate the experimental surface roughness (Ra) values, the RSM methodology has been adopted to model and analyze the machining parameters in diverse machining conditions. The RSM gives the reasonable mathematical response relationship among the desired response- and the independent input variables as follows. Here derivation

Considering (Y) =the response; x_i= (1,2,3…k) the coded-level of k-variables and b_0 = constant-term, where$b_i, b_{ii} b_{ij}$ are the coefficients of the linear-equation.

$$Y = b_0 + \sum_{i=1}^{k} (b_i x_i) + \sum_{i=1}^{k} (b_{ii} x_i x_i) + \sum_{i=1}^{k} \left(b_{ij} x_i x_j\right) \tag{7}$$

The nonlinear Eq. (7) is transformed into the linear through "logarithmic-transformation". The MINITAB-software is employed to conclude the coefficients of mathematical modeling to support the response. The predictable response is used in the generalized regression Eq. (7) as given in Eq. (8). The general second-order model is given below.

$$\begin{aligned} Y_1 = {}' b_0 + b_1 x_1 + b_2 x_2 + b_3 x_3 + b_4 x_4 + b_{12} x_1 x_2 + b_{23} x_2 x_3 + b_{14} x_1 x_4 + b_{24} x_2 x_4 + b_{13} x_1 x_3 \\ + b_{34} x_3 x_4 + b_{11} x_1^2 + b_{22} x_2^2 + b_{33} x_3^2 + b_{44} x_4^2, \end{aligned} \tag{8}$$

where Y_1 is the estimated-response based on second-order-equation.

The parameters $b_0 b_1 b_2 b_3 b_4 b_{12} b_{23} b_{23}$estimated by the method of least--squares. The coded-values of variables used in Eq (8) were obtained from the following transforming--equations:

$$x_1 = \frac{[\ln V - \ln (v)_{\text{centre}}]}{[\ln (v)_{\text{high}} - \ln (v)_{\text{centre}}]} \tag{9}$$

$$x_2 = \frac{[\ln F - \ln (f)_{\text{centre}}]}{[\ln (f)_{\text{high}} - \ln (f)_{\text{centre}}]} \tag{10}$$

$$x_3 = \frac{[\ln \text{D} - \ln (d)_{\text{centre}}]}{[\ln (d)_{\text{high}} - \ln (\text{d})_{\text{centre}}]} \tag{11}$$

$$x_4 = \frac{[\ln T - \ln (\text{t})_{\text{centre}}]}{[\ln (t)_{\text{high}} - \ln (\text{t})_{\text{centre}}]} \tag{12}$$

The data collected by the different experimental setups are considered for statistical analysis and constructs a numerical model to predict the surface roughness. First, ANOVA is employed to analyze the impact of processing parameters. Subsequently, predictions were developed to estimate surface roughness under different environmental conditions. The relationship between the calculated response factor and the various input constraints was quantified using Response Surface Methodology (RSM).

According to RSM (ANOVA table included), in Table 6 where SS is the adjusted sum of squares, Adj MS is the adjusted mean square. The P-value and the F-value are statistical measures used to assess the significance of the differences between group means. Residuals are the differences between the observed values and the predicted values from a statistical model. In this graph, all the experimental values are very close to the linear line. The residual analysis plots are given in Figure 9; the normal probability plot is important in residual analysis graphs because it allows to assess the assumption of normality for the residuals. Here, Figure 9(a) shows that the data points are placed near each other following the red-coloured straight line, which indicates normality in the data. The residuals versus fit plot gives residual analysis graphs as it helps identify patterns or deviations in the residuals relative to the predicted values. Figure 9(b) indicates that the residuals are randomly scattered on both sides of the zero residual line indicating constant variance. The histogram plot in residual analysis graphs helps visualize the distribution of residuals. It allows us to assess the assumption of normality and identify any deviations or outliers in the data. Figure 9(c) is the histogram for frequency distribution and this indicates the normality inside the data. The residuals versus order plot helps to identify patterns or trends in the residuals over the order of observations. It can reveal autocorrelation or time-dependent structure in the data. Figure 9(d) also validates the normality inside the data with a little bit of variance which is only for one data point.

Table 6 Analysis of variance

Source	DF	Adj SS	Adj MS	F-Value	P-Value
Model	9	164.324	18.2582	0.82	0.613
Linear	3	78.916	26.3053	1.18	0.366
Speed	1	2.714	2.7144	0.12	0.734
Feed rate	1	69.688	69.6883	3.13	0.107
Depth of cut	1	6.513	6.5132	0.29	0.601
Square	3	84.348	28.1159	1.26	0.339
Speed*Speed	1	4.282	4.2820	0.19	0.670
Feed rate*Feed rate	1	75.659	75.6594	3.39	0.095
Depth of cut*Depth of cut	1	0.376	0.3758	0.02	0.899
2-Way Interaction	3	1.061	0.3535	0.02	0.997
Speed*Feed rate	1	0.407	0.4068	0.02	0.895
Speed*Depth of cut	1	0.020	0.0198	0.00	0.977
Feed rate*Depth of cut	1	0.634	0.6339	0.03	0.869
Error	10	222.875	22.2875		
Lack-of-Fit	5	203.781	40.7561	10.67	0.011
Pure Error	5	19.094	3.8188		
Total	19	387.199			

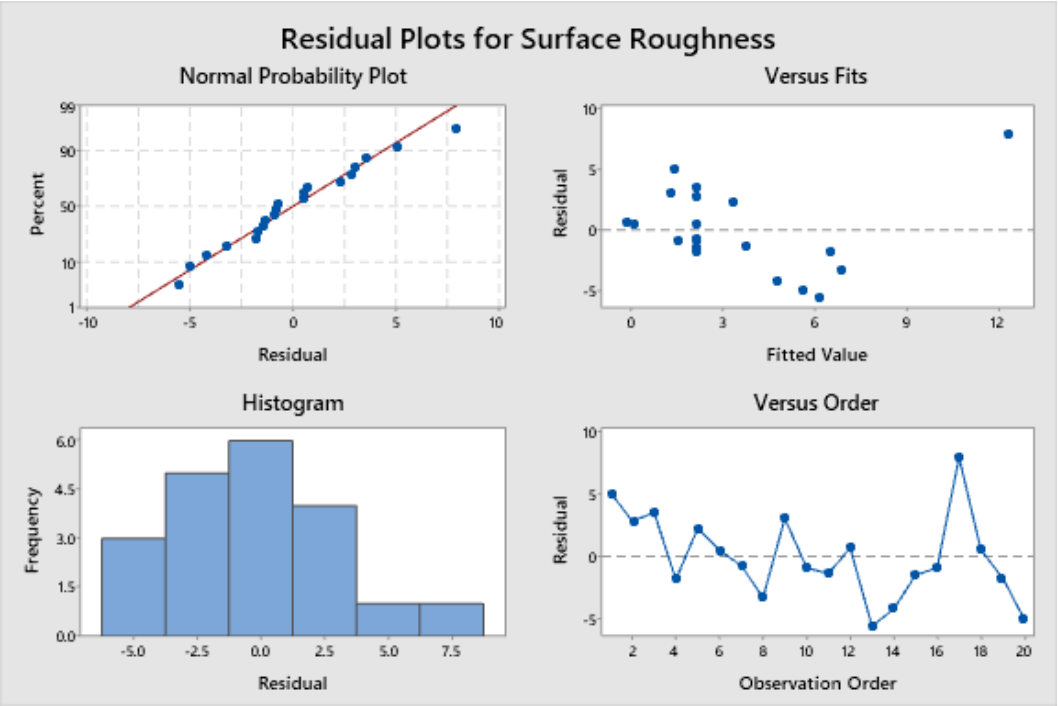

Figure 9. (a) Normal probability plot, (b) versus fits, (c) histogram, and (d)versus order

The following is the mathematical model established to investigate the impact of various cutting parameters on surface roughness:

$$\text{Surface Roughness} = 8.27 - 0.00199\ v - 10.1\ f - 1.96\ d + 0.0273\ t + 0.000001\ v\ 2 + 38.5\ f^2 + 0.195\ d^2 - 0.000049\ t^2 - 0.0011\ v{*}f + 0.00031\ v * d - 0.000031\ v * t + 3.41\ f * d + 0.0827\ f * t + 0.00966\ d * t \quad (13)$$

Based on the results obtained from various trials, the predicted mathematical model is utilized to calculate the surface roughness. These trials involve testing different combinations of cutting parameters and measuring the resulting surface roughness. By applying the established mathematical model to these experimental data points, the surface roughness values can be estimated for different sets of cutting parameters. This enables a better understanding of how changes in the cutting parameters affect the surface roughness during machining processes. Table 7 presents the experimental and predicted values, along with the corresponding percentage of error. Earlier, surface roughness values (Ra) obtained from the experimental trials are given in the third column of Table 7, whereas the fourth column represents the corresponding values obtained through an established mathematical model. The percentage of errors (ranges from -17.90% to 20.10%) shown in the fifth column of Table 7 qualifies the numerical predictive model in Eq. (13). The predicted values exhibit an average error of approximately 1.83% in dry, 2.37% in wet and 8.175% in cryogenic condition (Table 7), shows a close proximity in values.

Based on the information gathered from the relational factors, several conclusions can be drawn. The mathematical relationship is developed to predict the surface roughness (Ra) based on the given input constraints, such as spindle speed (N), feed rate (f), depth of cut (d), and temperatures (specifies the machining condition) for a given material. Based on Figure 10, the trials labelled 1 to 9 represent dry machining (D1 to D9). Similarly, trials labelled 10 to 18 represent wet machining (W1 to W9), and trials labelled 19 to 27 represent cryogenic coolant machining (C1 to C9). It can be observed that cryogenic coolant machining significantly decreases the surface roughness (Ra) values compared to dry and wet machining. This reduction in surface roughness is attributed to the minimized fiber pullout and decreased buckling failure during cryogenic machining (discussed earlier). Figure 11 presents the predicted and experimental values for surface roughness. According to the SEM results obtained from cryogenic machining conditions, there is a notable reduction in fiber pullout (84 µm to 34 µm) and delamination, leading to an improvement (25.21%) in surface roughness value.

Table 7. Experimental and predicted surface-roughness values

Sl. No.	Trial No.	Experiment value (Ra)	Predicted value (Ra)	% of error	Remarks
1	D1	5.074	4.56	11.27	Higher
2	D2	5.692	6.584	-13.55	Lower
3	D3	5.328	4.951	7.61	Higher
4	D4	5.751	6.213	-7.44	Lower
5	D5	4.958	4.625	7.2	Higher
6	D6	6.436	6.044	6.49	Higher
7	D7	5.11	6.126	-16.59	Lower
8	D8	4.58	3.952	15.89	Higher
9	D9	6.286	5.952	5.61	Higher
10	W1	4.958	4.242	16.88	Higher
11	W2	5.269	6.146	-14.27	Lower
12	W3	5.126	4.449	15.22	Higher
13	W4	5.512	6.545	-15.78	Lower
14	W5	4.648	5.216	-10.89	Lower
15	W6	5.95	5.622	5.83	Higher
16	W7	5.101	4.965	2.74	Higher
17	W8	4.265	4.154	2.67	Higher
18	W9	5.901	4.96	18.97	Higher
19	C1	3.985	4.854	-17.9	Lower
20	C2	4.213	3.654	15.3	Higher
21	C3	4.124	3.784	8.99	Higher
22	C4	4.289	3.927	9.22	Higher
23	C5	4.098	3.625	13.05	Higher
24	C6	4.258	3.658	16.4	Higher
25	C7	4.085	3.66	11.61	Higher
26	C8	3.925	3.268	20.1	Higher
27	C9	3.826	3.952	-3.19	Lower

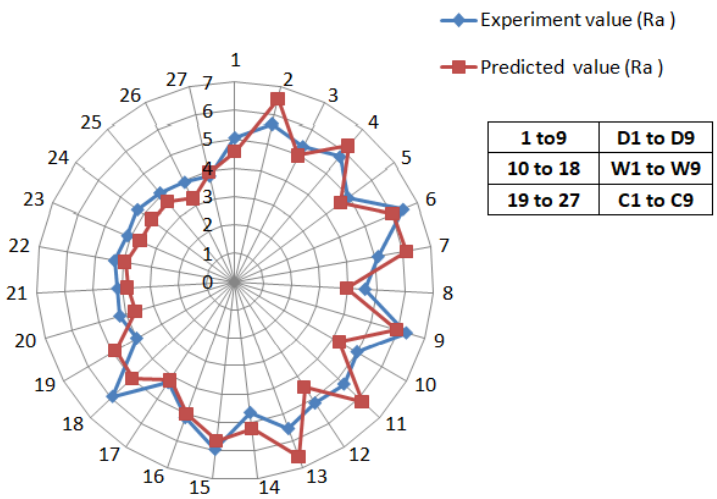

Figure 10. Prediction vs experiment for surface roughness,

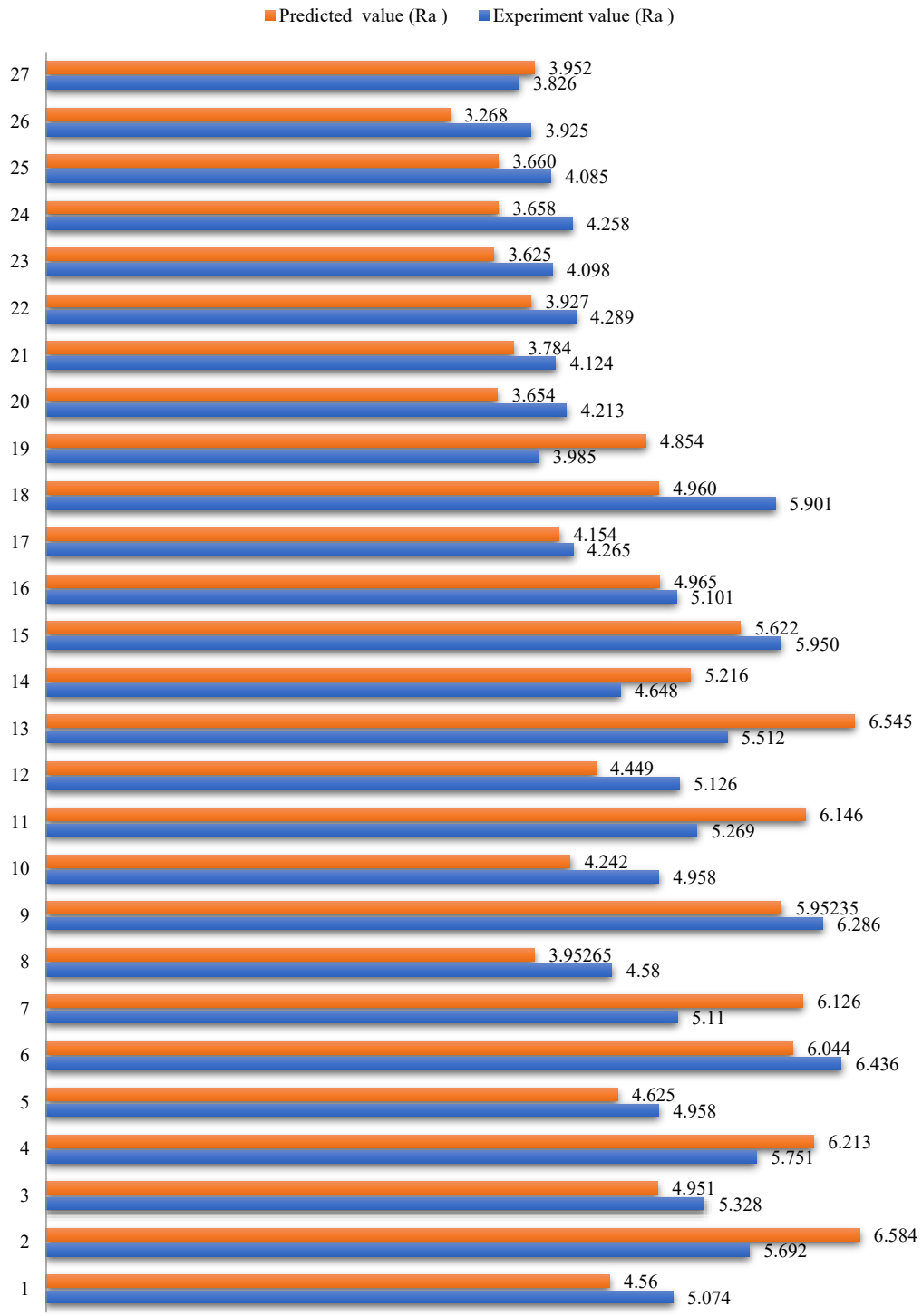

Figure 11. Variation of surface roughness

6.0 CONCLUSIONS

In this paper, the Taguchi optimization approach was employed to optimize the turning process of Unidirectional E-Glass Fiber Reinforced Polymer (UD-EGFRP) composite using a Polycrystalline Diamond (PCD) tool. Primarily, the focus was on the optimization of machining parameters for UD-EGFRP under diverse machining conditions, for example, dry, wet and cryogenic environments. The followings are the summary of the experimental findings obtained from this study.

i. When analyzing the effects of different lubrication methods (dry, wet, and cryogenic machining) on surface roughness, it was observed that cryogenic machining resulted in a significant improvement of 25.21%.
ii. Some potential factors contributing to the enhanced surface roughness in cryogenic machining could include reduced heat generation, improved chip evacuation, decreased tool wear and compressive residual stress.

iii. In dry machining of UD-EGFRP, the issue of fiber pullout is exacerbated, leading to rough surface roughness, increased tool wear, and delamination.
iv. In cryogenic-assisted machining conditions, the occurrence of fiber pullout is significantly reduced from 84 μm to 34 μm.
v. After the machining process, liquid nitrogen evaporates and mixes with the surrounding environment. As a result, nitrogen is obtained from the environment and further blends with the surroundings. This process does not generate any hazardous waste, thus merely preferable over others.
vi. Furthermore, a mathematical relationship has been developed to predict the surface roughness, which ultimately helps the machinist before its actual machining.

Finally, it can be concluded that cryogenic machining involves the application of a cooling medium, typically liquid nitrogen, to reduce the temperature during the cutting process. This cooling effect can have several benefits, including reducing tool wear, minimizing residual stresses, and improving surface quality.

7.0 FUTURE SCOPE

Machinability tests can be extended to find out the material removal rate (MRR) using various fiber orientations. Additionally, fiber fracture analysis can be conducted to further examine and investigate the process better. Further, this study can be planned to make aid for Bi or MD-EGFRP composite parts and/or with different tools to explore new possibilities of the results in this direction.

8.0 ACKNOWLEDGEMENT

We sincerely thank the editors and reviewers for their time, expertise, and invaluable input. Their efforts have been instrumental in improving the quality and rigor of our research, and we are truly grateful for their support throughout the review process. We also would like to thank the research supervisor and mentors for their valuable suggestions towards this research work.

9.0 REFERENCES

[1] M. Slamani, J-F. Chatelain "A review on the machining of polymer composites reinforced with carbon (CFRP), glass (GFRP), and natural fibers (NFRP)" *Discover Mechanical Engineering*, vol. 2, no. 4, p. 4, 2023.
[2] M. Gupta, and S. Kumar, "Investigation of surface roughness and MRR for turning of UD- GFRP using PCA and Taguchi method," *Engineering Science and Technology, an International Journal*, vol. 18, issue 1, March, pp. 70-81, 2015.
[3] S. Kumar, Meenu, and P.S. Satsangi, "Multiple-response optimization of turning machining by the Taguchi method and the utility concept using unidirectional glass fiber-reinforced plastic composite and carbide (k10) cutting tool," *Journal of Mechanical Science and Technology*, vol. 27, no. 9, pp. 2829–2837, 2013.
[4] E.S. Lee, "Precision machining of glass fibre reinforced plastics with respect to tool characteristics," *The International Journal of Advanced Manufacturing Technology*, vol. 17, no. 11, pp. 791-798, 2001.
[5] M. Henerichs, R. Voß, and F. Kuster, "Machining of carbon fiber reinforced plastics: Influence of tool geometry and fiber orientation on the machining forces," *CIRP Journal of Manufacturing Science and Technology*, vol. 9, pp. 136–145, 2015.
[6] J.P. Davim, and P. Reis, "Multiple regression analysis (MRA) in modelling milling of glass fibre reinforced plastics (GFRP)," *International Journal of Manufacturing Technology and Management*, vol. 6, no. 1/2, pp. 185–185, 2004.
[7] C. Cheng-Hung, J. Shiou-Yun, and L. Cheng-Jian, "Prediction and analysis of the surface roughness in CNC end milling using neural networks," *Applied Science*s, vol.12, no. 1, p. 393, 2022.
[8] J.P. Davim, and F. Mata, "New machinability study of glass fibre reinforced plastics using polycrystalline diamond and cemented carbide (K15) tools," *Materials and Design*, vol. 28, no. 3, pp. 1050–1054, 2007.
[9] S. Arul, D.S. Raj, and L. Vijayaraghavan, "Modeling and optimization of process parameters for defect tolerance drilling of GFRP Composites," *Materials and Manufacturing Processes*, vol. 21, pp. 357–365, 2006.
[10] B. Işık, and A. Kentli, "Multicriteria optimization of cutting parameters in turning of UD-GFRP a trial considering sensitivity," *The International Journal of Advanced Manufacturing Technology*, vol. 44, no. 11- 12, pp. 1144–1153, 2009.
[11] Mohd. Javaid, A. Haleem, R. P. Singh, S. Khan, and R. Suman "Sustainability 4.0 and its applications in the field of manufacturing," *Internet of Things and Cyber-Physical Systems,* vol. 2, pp. 82–90, 2022.
[12] H. Hegab, U. Umer, M. Soliman, and H.A. Kishawy, "Effects of nano-cutting fluids on tool performance and chip morphology during machining Inconel 718," *International Journal of Advanced Manufacturing Technology,* vol. 96, pp. 3449-3458, 2018.
[13] S. Spagnuolo, Z. Rinaldi, J. Donnini, and A. Nanni "Physical, mechanical and durability properties of GFRP bars with modified acrylic resin (modar) matrix," *Composite Structures*, vol. 262, p. 11355, 2021.
[14] S.A. Ashrafi, P. W. Miller, K. M. Wandro and D. Kim "Characterization and effects of fiber pullouts in hole quality of carbon fiber reinforced plastics composite," *Materials*, vol. 9, pp. 828, 2 of 12, 2019.
[15] T. Wan, X. Chen, C. Li, and Y. Tang, "An on-line tool wear monitoring method based on cutting power," In 2018 IEEE 14th International Conference on Automation Science and Engineering (CASE), 2018, pp. 205–210.
[16] I. Singh, N. Bhatnagar, and P. Viswanath, "Drilling of unidirectional glass fiber reinforced plastics: Experimental and finite element study," *Materials and Design*, vol. 29, pp. 546–553, 2008.
[17] K. Palanikumar, "Experimental investigation and optimization in drilling of GFRP composites," *Measurement*, vol. 44, pp. 2138–2148, 2011.
[18] U. Koklu, S. Morkavuk, C. Featherston, M. Haddad, D. Sanders, et al., "The effect of cryogenic machining of S2 glass fibre composite on the hole form and dimensional tolerances," *International Journal of Advanced Manufacturing Technology,* vol. 115, pp. 125–140, 2021.

[19] I. M. Alarifi "A review on factors affecting machinability and properties of fiber-reinforced polymer composites," *Journal of Natural Fibers*, vol. 20, no. 1, 21543, 2023.
[20] H. Naresh, P. C. Prasad "Investigating machinability performances of UD-GFRP rods under green machining and cryogenic machining environment by response surface methodology," *Journal of Mechanical Engineering Research and Developments*, vol. 44, no. 11, pp. 21-33, 2021.
[21] H. Naresh, and P. C. Prasad "Lathe parameters optimization for UD-GFRP composite part turning with PCD tool by Taguchi method," *INCAS Bulletin*, vol. 12, issue 4, pp. 135 – 144, 2020.
[22] H. Naresh, and P. C. Prasad "Optimization of parameters in turning of UD-GFRP cryogenic condition with Taguchi method," *International Research Journal of Engineering and Technology* (IRJET), vol. 08, no. 7, pp.4093-4099, 2021.
[23] B. Yang, H. Wang, K. Fu and C. Wang "Prediction of cutting force and chip formation from the true stress–strain relation using an explicit FEM for polymer," *Polymers*, vol. 14, no. 1, p. 189, 2022.
[24] M. Elfarhani, F. Guesmi, A. Mkaddem, S. Ghazali, S. Rubaiee and A. Jarraya "Thermal aspects in edge trimming of bio-filled GFRP: Influence of fiber orientation and silica sand filler in heat generation," *Materials*, vol. 15, pp. 4792, 2022.
[25] I. Shyha, D. Huo, P. Hesamikojidi, H. Eldessouky, and M.A. El-Sayed, "Performance of a new hybrid cutting-abrasive tool for the machining of fibre reinforced polymer composites," *International Journal of Advanced Manufacturing Technology,* vol. 112, pp. 1101–1113, 2021.
[26] P. B. Patole1, and V. V. Kulkarni "Prediction of surface roughness and cutting force under MQL turning of AISI 4340 with nano fluid by using response surface methodology," *Manufacturing Review*, vol. 5, pp. 1-12, 2018.